I-22-11
E6272

NASA Contractor Report 187140

Physical Optics for Oven-Plate Scattering Prediction

J. Baldauf
University of Illinois
Urbana, Illinois

and

K. Lambert
Analex Corporation
Brook Park, Ohio

July 1991

NASA
National Aeronautics and
Space Administration

PHYSICAL OPTICS FOR OVEN-PLATE SCATTERING PREDICTION

J. Baldauf[*]
University of Illinois
Urbana, Illinois 61801

and

K. Lambert
Analex Corporation
Brook Park, Ohio 44124

ABSTRACT

This report describes an oven assembly design, which will be used to determine the effects of temperature on the electrical properties of materials which are used as coatings for metal plates. Experimentally, these plates will be heated to a very high temperature in the oven assembly, and measured using a microwave reflectance mesurement system developed for the NASA Lewis Research Center, Near-Field Facility. One unknown in this measurement is the effect that the oven assembly will have on the reflectance properties of the plate. Since the oven will be much larger than the plate, the effect could potentially be significant as the size of the plate becomes smaller. Therefore, it is necessary to predict the effect of the oven on the measurement of the plate. This report will describe a method for predicting the oven effect, compare the theoretical oven effect to experimental results of the oven material, and describe the computer code which is used to predict the oven effect.

I. INTRODUCTION

An oven assembly design, similar to the one shown in figure 1, will be used to determine the effects of temperature on the electrical properties of materials which are used as coatings for metal plates. Experimentally, these plates will be heated to a very high temperature in the oven assembly, and measured using a microwave reflectance measurement system developed for the NASA Lewis Research Center, Near Field Facility (ref. 1). The oven is to be constructed of Lockheed, High Thermal Performance, rigid, composite fiber, ceramic insulation (HTP-6-22). This material is similar to that which is used to produce the tiles that form the heat shield for the Space Transportation System, shuttle orbiters. This material has a relative dielectric constant of about 1.07 (refractive index of 1.03) and a very small loss tangent. Therefore, the oven assembly should have very little effect upon the measurement of the plate. Since the oven will be much larger than the plate though, the effect could potentially be significant as the size of the plate becomes smaller. Therefore, it is necessary to predict the effect of the oven on the measurement of the plate. This report will describe a method for predicting the oven effect, compare the theoretical oven effect to experimental results of the oven material, and describe the computer code which is used to predict the oven effect.

---

[*]Summer Student Intern at NASA Lewis Research Center.

II. THE PHYSICAL OPTICS TECHNIQUE

The Physical Optics technique (PO) is based on equivalence principle and radiation scattering of the equivalent Huygen's sources. Figure 2 shows how the original scattering problem can be replaced by an equivalent auxiliary problem which consists of free space radiation of currents in space. This is easy to solve once the currents are known (2.1), but it is a difficult procedure to determine the equivalent currents exactly. Therefore the PO method will provide us with an easy, relatively accurate, method of approximating these surface currents.

$$E^s = -\nabla \times F + \frac{1}{j\omega \varepsilon_0} \nabla \times \nabla \times A \tag{2.1a}$$

$$A = \frac{1}{4\pi} \int_{s'} \int \frac{J_s e^{-jk}|r - r'|}{|r - r'|} dS' \tag{2.1b}$$

$$F = \frac{1}{4\pi} \int_{s'} \int \frac{K_s e^{-jk}|r - r'|}{|r - r'|} dS' \tag{2.1c}$$

where A and F are the magnetic and electric potentials and J_s and K_s are the electric and magnetic equivalent currents. S' is the surface of the scatterer with the physical body of the scatterer removed.

The PO technique is a high-frequency method (the accuracy increases as the wavelength of the radiation goes to zero). Therefore, this technique is best suited for electrically large scatterers which have smooth surface variations. For the case of the oven, the surfaces are flat and on the order of 15 to 20 wavelengths in length. PO, therefore, should produce good results for a problem of this kind. PO has the advantage that it is a simple, fast way to determine scattering from the complex bodies. In fact, it would be very difficult to apply any other type of numerical technique to solve for the scattering from such a large structure as the oven assembly.

For the scattering computations to be performed, the electric fields very far from the scatterer are desired. In this case, far field approximations can be applied to simplify (2.1) to yield (2.2).

$$E^s = \frac{e^{-jk_0 r}}{4\pi r} (-jk_0) \int_{s'} \int [\eta J_s(r') + K_s(r') \times \hat{k}] e^{jk \cdot r'} dS' \tag{2.2}$$

k = the wavevector in the direction of propagation of the outgoing wave

$$|k| = k_0 = \frac{2\pi}{\lambda}.$$

η = free space impedance = 120π.

From this equation, the equivalent currents are needed to obtain the far electric fields. The PO approximation for obtaining these currents assumes that the fields around the body behave as geometric optics (GO) rays which all obey Snell's law at the surface of the scatterer. The regions which are not directly illuminated or "lit" by the incident field are assumed to have zero

surface currents. The currents can then be evaluated using GO approximations (2.3).

$$E^i + E^s = E^t; \quad E^s \approx E^r$$

$$H^i + H^s = H^t; \quad H^s \approx H^r \tag{2.3}$$

E^s and H^s are the scattered fields as defined in figure 2. E^i and H^i are the incident fields as defined in figure 2, and E^r and H^r are the GO reflected fields at the surface of the scatterer, (shown in fig. 3). The reflected fields can then be determined by (2.4).

$$E_{TE}^r = \Gamma_{TE} E_{TE}^i; \quad E_{TE}^r = -\Gamma_{TE} H_{TE}^i$$

$$E_{TM}^r = \Gamma_{TM} E_{TM}^i; \quad H_{TM}^r = -\Gamma_{TM} H_{TM}^i \tag{2.4}$$

Γ_{TE} and Γ_{TM} are the transverse electric and transverse magnetic Fresnel reflection coefficients. The equivalent surface currents can then be determined by (2.5).

$$J_s = \hat{n} \times (H^s + H^i)$$

$$K_s = (E^s + E^i) \times \hat{n} \tag{2.5}$$

Substituting the approximate expressions for the scattered electric and magnetic fields into this expression will result in the PO approximate current expressions. The scattered far fields can be determined, and they can be expressed in terms of a parameter commonly used in microwave reflectivity work known as Radar Cross Section (RCS). This is defined as (2.6).

$$\sigma = 4\pi r^2 \frac{|E^s|^2}{|E^i|^2} \tag{2.6}$$

This parameter is based on the radar equation (2.7).

$$P_r = P_t \frac{A_{er} A_{et} \sigma}{4\pi r^4 \lambda^2} \tag{2.7}$$

where

P_r = power received by the radar

P_t = power transmitted by the radar

A_{er} = effective area of the receiving antenna

A_{et} = effective area of the transmitting antenna

λ = wavelength of the radiation

r = distance from the scatterer to the radar antenna.

3

The RCS is a commonly used measure of the far field reflectivity of scattering bodies. Note that when the plate size becomes small, the relative effect of the oven is large, and it is difficult to determine what is happening to the reflectance of the plate. Note also, that the oven is much larger than the quiet zone and the "tapering" of the magnitude of the incident fields from the half scale reflector can be accounted for in the PO model, although it is difficult to exactly account for this effect.

III. THE INVERSE PROBLEM

Observing the effects of temperature on the radar cross section of the plates gives some insight into what is happening to the material coating. Even more insightful though, would be to determine the reflection coefficient at the surface of the material coating on the plate. Assuming there is little warping of the material and the relative dimensions of the problem are known, some information about the reflection coefficient can be determined. This section deals with how to determine this information from the reflected radar signal and radar cross section.

The multiple layer reflectance coefficient for the configuration given in figure 4 is given in (3.1). This is a recursive formula for the overall reflection coefficient. The reflection coefficients, R_{12}, R_{23}, etc., are for a wave propagating from one infinite medium into another. From (3.1), an expression for the reflection coefficient at the surface of the material can be obtained (3.3). From the reflection coefficient at the surface of the material, some information about permittivity and permeability of the material can be determined.

$$\tilde{R}_{12} = R_{12} + \frac{T_{12}\tilde{R}_{23}T_{21}e^{-j2k_{2z}(d_2-d_1)}}{1 - R_{21}\tilde{R}_{23}e^{-j2k_{2z}(d_2-d_1)}} \qquad (3.1)$$

R_{12} = the reflection coefficient of a wave going from medium one to medium two, both mediums extending to infinity.

T_{12} = $1 + R_{12}$ = the transmission coefficient of a wave going from medium one to medium two, where the media are infinite.

$\tilde{R}_{23}$ = reflection coefficient at the dielectric interface between mediums one and two, where the media are finite.

k_2z = the z-component of the wave vector k_2 in the medium two

$$R_{21} = -R_{12}$$
$$T_{21} = 1 + R_{21}$$

and where

$$R_{12}^{TE} = \frac{\mu_2 k_{1z} - \mu_1 k_{2z}}{\mu_2 k_{1z} + \mu_1 k_{2z}} \qquad (3.2a)$$

$$R_{12}^{TM} = \frac{\varepsilon_2 k_{1z} - \varepsilon_1 k_{2z}}{\varepsilon_2 k_{1z} + \varepsilon_1 k_{2z}}. \qquad (3.2b)$$

4

In order to determine the behavior of the coating on the plate, $\tilde{R}_{23}$ can be determined by using the following formula derived from (3.1).

$$\tilde{R}_{i+1,i+2} = \frac{\left[\tilde{R}_{i,i+1} - R_{i,i+1}\right]e^{j2k_{i+1,z}(d_{i+1}-d_i)}}{\left[R_{i+1,i}\left(\tilde{R}_{i,i+1} - R_{i,i+1}\right) + T_{i,i+1}T_{i+1,i}\right]} \tag{3.3}$$

It seems, therefore, that information about the reflection coefficient of the material coating can be determined regardless of the effects of the oven walls using this procedure.

IV. IMPLEMENTING THE PO SCHEME

The problem of oven scattering at broadside incidence can be simplified within the PO approximation to that of a plate scatterer with several differ-ent reflection coefficients over its surface corresponding to (1) the region with the plate behind it, (2) the region with no plate behind it as shown in figure 5. For broadside scattering, the expression for the scattered far-fields (2.1) further simplifies to (4.1).

$$E^s = \frac{e^{-jk_0r}}{4\pi r}(-jk_0) \sum_{\text{subareas}} \left[\eta J_s(r_{\text{subarea}}') + K_s(r_{\text{subarea}}')\times\hat{k}\right]e^{jk\cdot r'}\Delta s_{\text{subarea}} \tag{4.1}$$

where
k = the wavevector in the direction of propagation of the outgoing wave

$$|k| = k_0 = \frac{2\pi}{\lambda}$$

and
η = free space impedance = 120π.

The tapering of the magnitude of the incident fields which is evident in the plot shown in figure 6 and is discussed in reference 1, can be taken into account by subdividing the region of the face of the oven into small subsec-tions as shown in figure 7. On each subsection, the incident fields are calculated assuming parabolic taper of the incident fields assuming on the near-field experimental data. The contribution to the scattered far fields from each subsection can then be summed to obtained the total scattered fields.

Since we know that the contribution from the regions (2) and (3) should be constant with temperature, the contribution from region (1) can be obtained, and the reflection coefficient on the surface of the material coating can then be obtained. From (3.2), we can obtain this reflection coefficient once the scattered electric fields from region (1) and the incident fields are known. Results will be shown in the next section which will demonstrate the validity of the PO scattering solution for the oven. Unfortunately, an experiment to determine the validity of the plate reflection coefficient extraction method from was not performed, and the details for the theoretical procedure have not been included.

5

V. COMPARISON OF THEORY WITH EXPERIMENTAL RESULTS

In order to determine the validity of the computer model derived from the PO formulation which is used to predict the scattering from the plate-oven system, experiments have been performed with which we will compare our computer model's results. The experimental results were obtained and described using the experimental microwave reflectivity measurement setup in the near-field range shown in figure 8 and described in reference 2. This is the same setup to be used in the plate-oven measurements. Several different configurations were measured and compared to the computed results: (1) a plate by itself, (2) a piece of shuttle tile material by itself at broadside incidence, (3) a piece of shuttle tile material at edge incidence, and (4) a piece of shuttle tile material with a plate behind it at broadside incidence for both the plate and the shuttle tile material. The comparisons between the experimental and computed results are shown in figures 9 to 13. As can be seen from these figures, the agreement between experimental results and the theoretical results is good. Notice, however, that the dielectric constant appears to be different when the electromagnetic waves are propagating in different directions in the shuttle tile material (figs. 10 to 12). The actual relative dielectric constant in one direction appears to be 1.073 (fig. 12) while in the other direction it appears to be 1.094 (figs. 10 and 11).

Figures 14 to 19 show the theoretical effect of the oven on the scattering from plates ranging 2 by 2 to 10 by 10 in. Though there are no experimental results to compare with these results, the good agreement with experiment that the single plate and dielectric had provides us with some confidence that these theoretical predictions are valid.

CONCLUSIONS

From the comparison of the experimental results and the theoretical results formulated with the PO approximation, the PO approximation is shown to be a good method for predicting the effect of the scattering from a plate within the oven. Though there is no exact way of predicting the scattering from the oven and plate because of their large size, the PO approximation provides us the usual results. From these results we can see that the oven can produce some noticeable effects on small plates, and therefore, large plates (10 by 10 in.) should be used for measurements in the oven whenever this is possible. Also of some interest is the fact that the apparent dielectric constant for the waves incident broadside of the shuttle tile material and incident on the edge of the shuttle tile material suggests that the tile material is anisotropic. In some situations, this could be a problem with regards to the prediction of the effect of the oven on the scattering of the plate. Therefore, this should be kept in mind when estimating the scattering from the oven-plate system.

REFERENCES

1. Lambert, K.M.: Measured Performance of the Half-Scale Accurate Antenna Reflector. NASA CR-187047, 1991.

2. Lambert, K.M.: Description and Operation of a Microwave Reflectance Measurement System. NASA CR–187063, 1991.
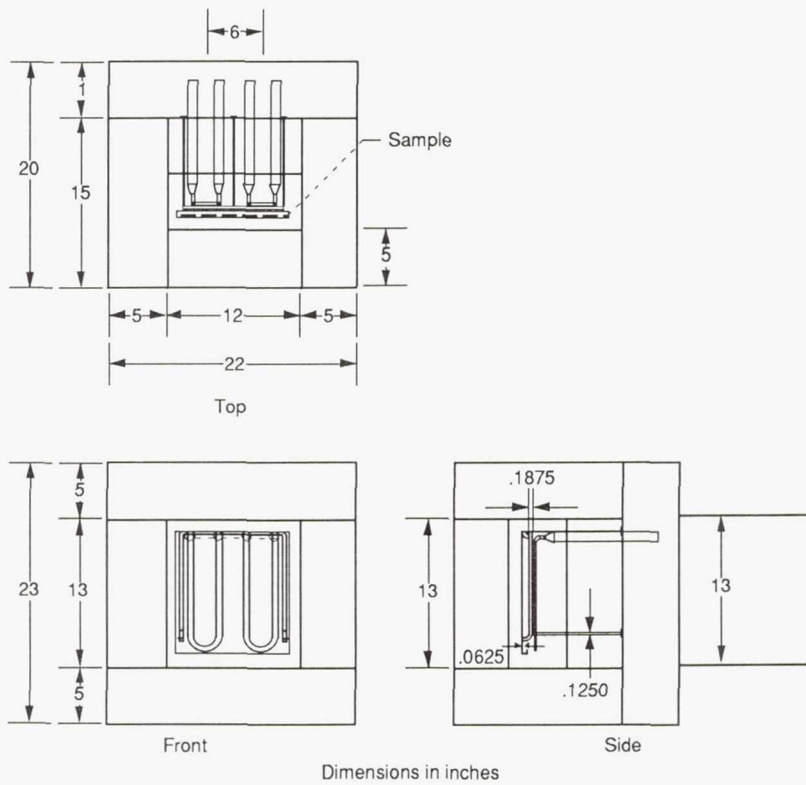

Figure 1.—Typical oven assembly to be placed in the near field for high temperature measurements. Top, front, and side views.
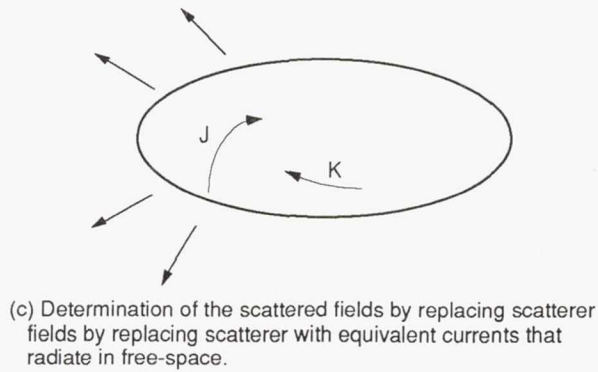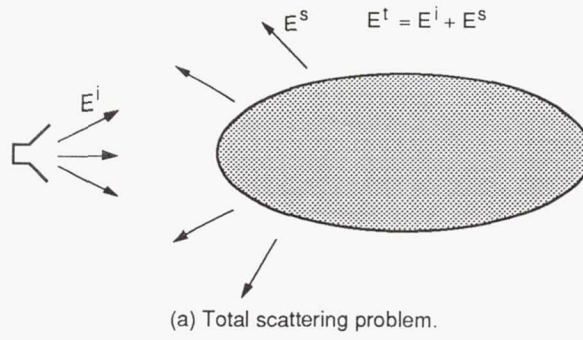
E^s $E^t = E^i + E^s$

E^i

(a) Total scattering problem.

E^i

(b) Determination of the incident fields by removing scatterer.

J

K

(c) Determination of the scattered fields by replacing scatterer fields by replacing scatterer with equivalent currents that radiate in free-space.

Figure 2.—Scatterer replaced by its equivalent currents.

E^r_{TE} $\hat{n}$ E^i_{TE}

E^r_{TM} θ^i E^i_{TM}

θ^r

$\theta^i = \theta^r$
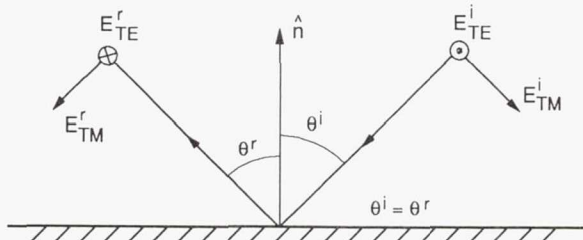
Figure 3.—Electric fields reflected at the surface of a scatterer.

$\hat{n}$

θ^r θ^i

ε_1 $z = -d_1$
ε_2 $z = -d_2$
ε_3

$z = -d_3$
ε_4 $z = -d_4$

ε_{N-1} $z = -d_{N-1}$
ε_N
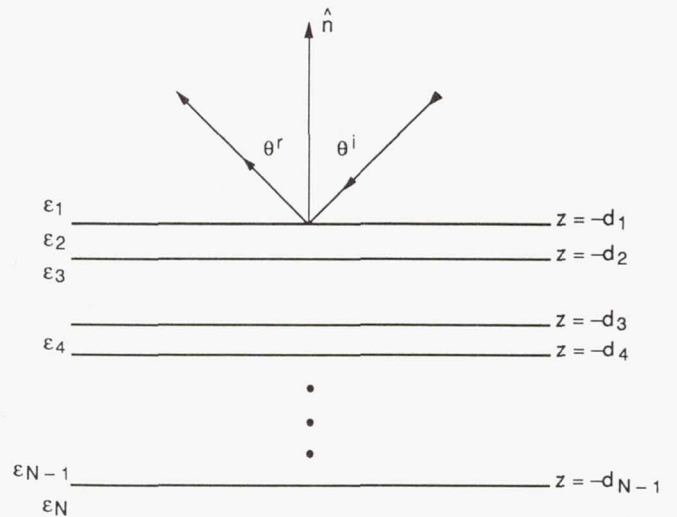
Figure 4.—Incident transverse electric and magnetic fields on a multilayer material coating.

8
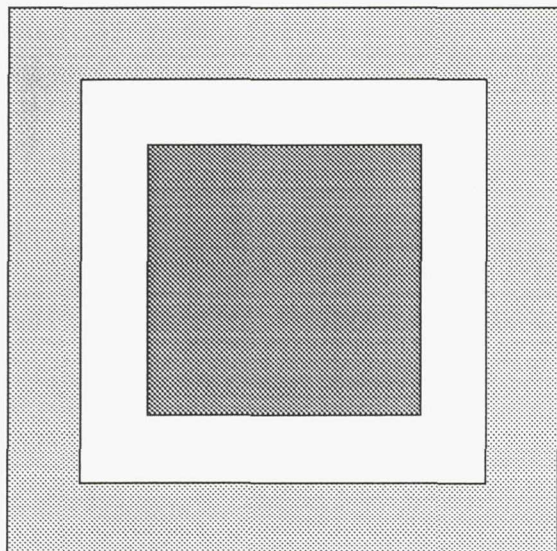
Figure 5.—Front face of the oven characterized by different material properties and reflection coefficients.
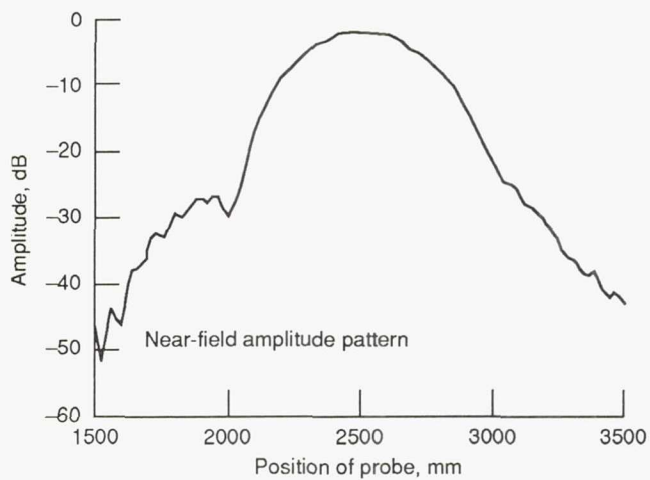
Figure 6.—Tapering of the incident fields on the target which are radiated from the half scale precision reflector antenna. Frequency, 10 GHz; wavelength, 30 mm; scan axis, horizontal.
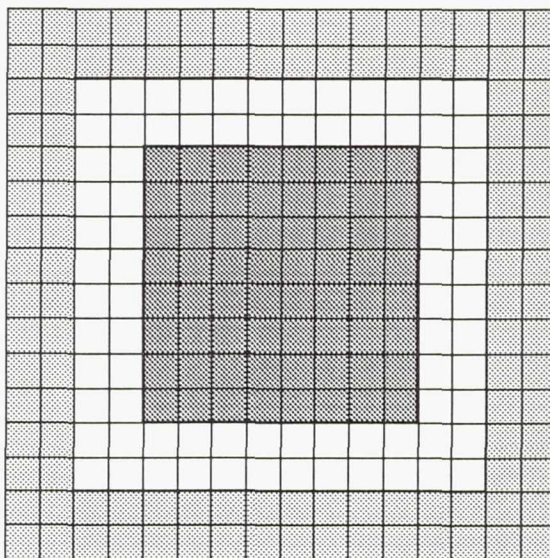
Figure 7.—Front face of the oven dividend into small subsections for numerical integration.
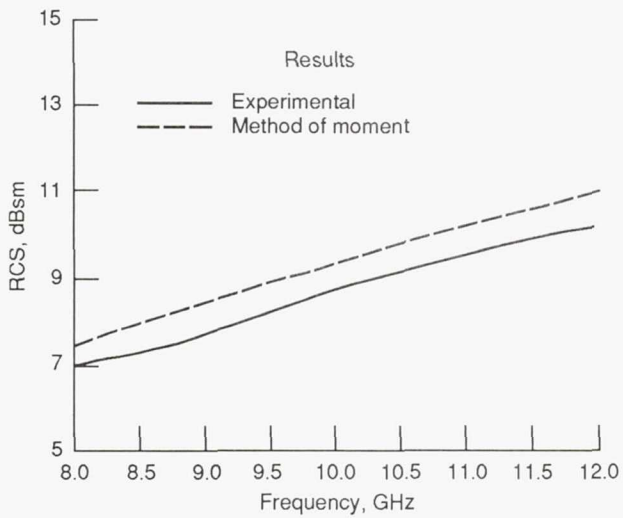
9
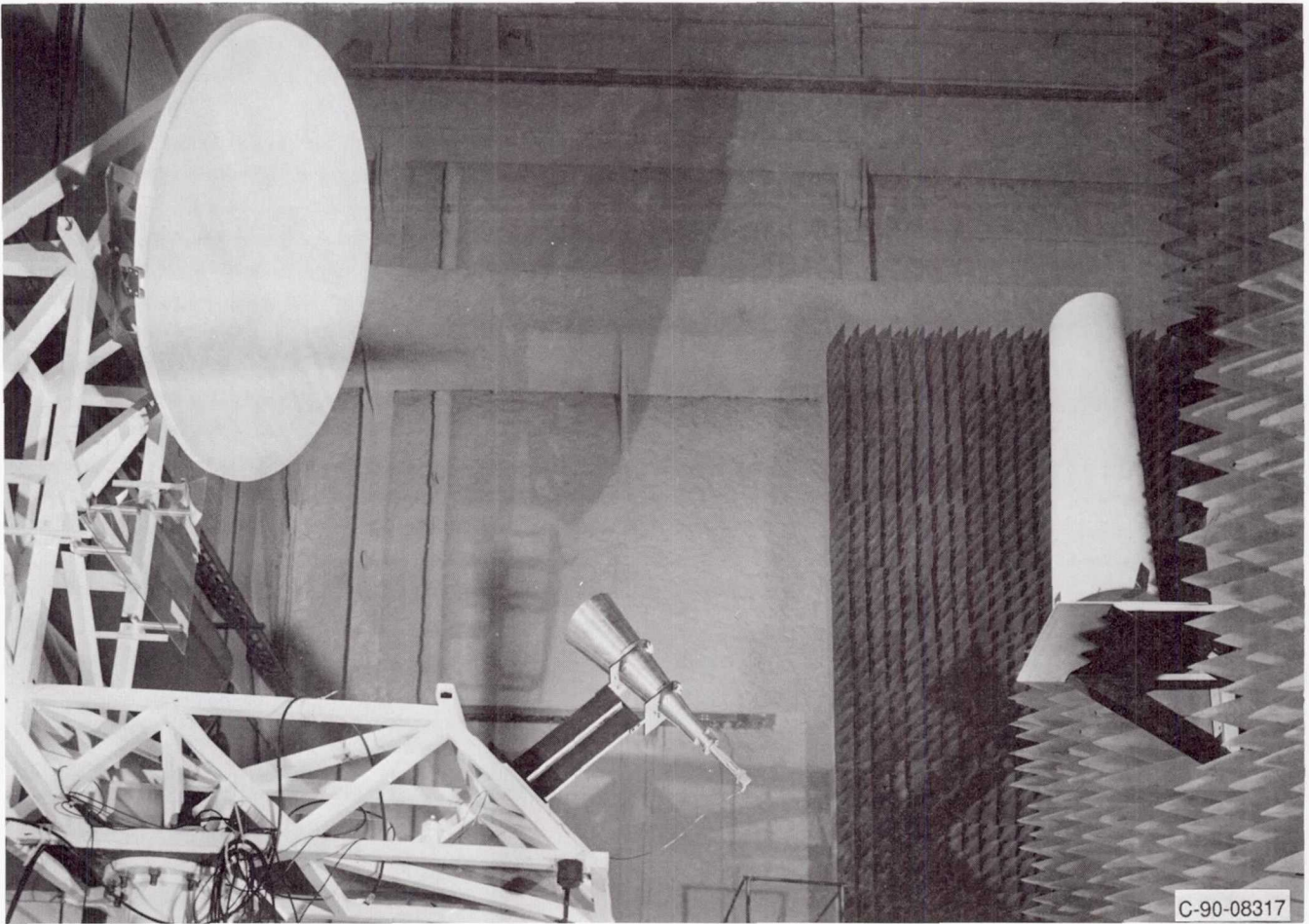
Figure 8.—Experimental setup in the near field range.

Figure 9.—Radar Cross Section (RCS) of an uncoated
metal plate 5 in. high by 8 in. wide.
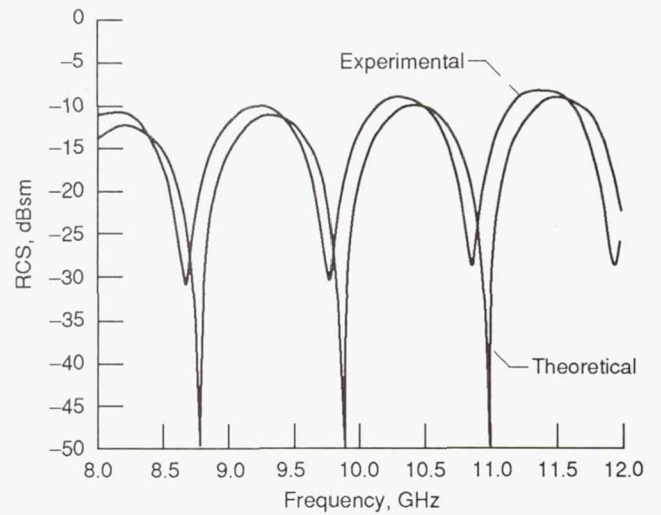
Figure 10.—Theoretical and experimental Radar Cross
Section (RCS) of shuttle tile material 5 3/16 in. thick,
10 in. wide, and 11 in. high at broadside incidence.
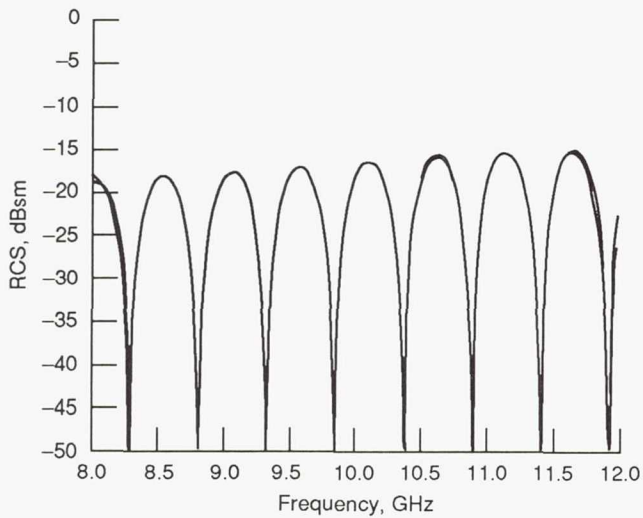The theoretical dielectric constant is 1.074.

10

Figure 11.—Theoretical and experimental Radar Cross
Section (RCS) of a piece of shuttle tile material 5 3/16
in. thick, 10 in. wide, and 11 in. high at edge, on
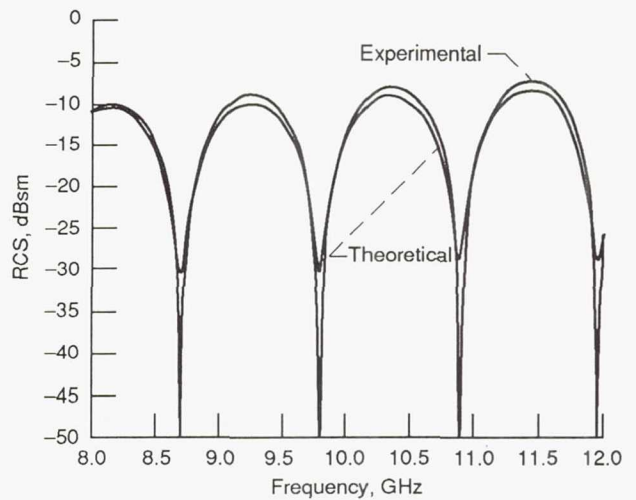incidence. The theoretical dielectric constant is 1.074.

Figure 12.—Theoretical and experimental Radar Cross
Section (RCS) of a piece of shuttle tile material 5 3/16 in.
thick, 10 in. wide, and 11 in. with a plate 5 in. high by 8
in. wide behind it at broadside incidence. The theoretical
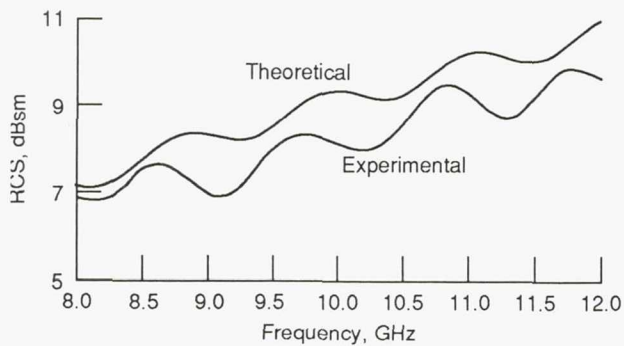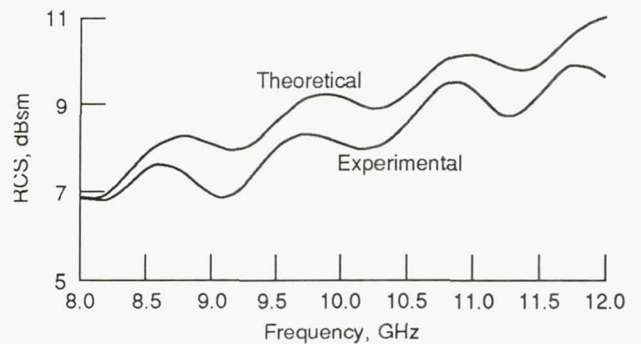dielectric constant is 1.093.

Figure 13.—Theoretical and experimental Radar Cross
Section (RCS) of a piece of shuttle tile material 5 3/16
in. thick, 10 in. wide, and 11 in. with a plate 5 in. high by
8 in. wide behind it at broadside incidence. The theo-
retical dielectric constant is 1.074.

Figure 14.—Theoretical and experimental Radar Cross
Section (RCS) of a piece of shuttle tile material 5 3/16
in. thick, 10 in. wide, and 11 in. with a plate 5 in. high by
8 in. wide behind it at broadside incidence. The theo-
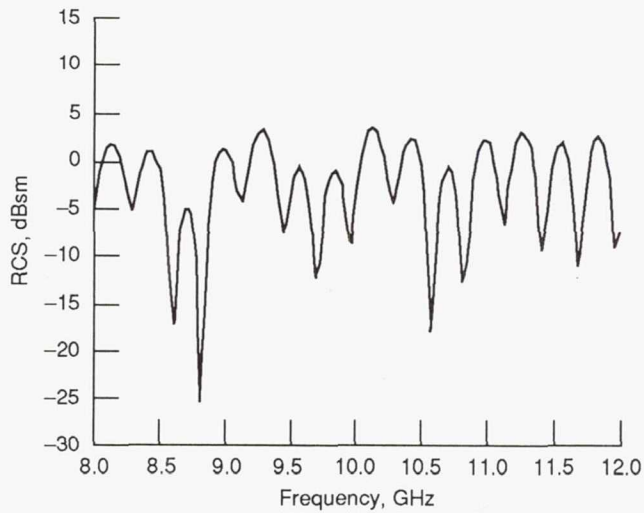retical dielectric constant is 1.094.

11

Figure 15.—Theoretical Radar Cross Section (RCS) of a
piece of shuttle tile material 5 3/16 in. thick, 10 in. wide,
and 11 in. with a plate 2 in. high by 2 in. wide behind it
at broadside incidence. The theoretical dielectric
constant is 1.093.

Figure 16.—Theoretical Radar Cross Section (RCS) of a
piece of shuttle tile material 5 3/16 in. thick, 10 in. wide,
and 11 in. with a plate 4 in. high by 4 in. wide behind it
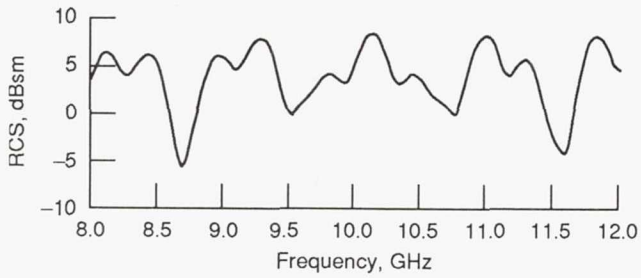at broadside incidence. The theoretical dielectric
constant is 1.093.

Figure 17.—Theoretical Radar Cross Section (RCS) of a
piece of shuttle tile material 5 3/16 in. thick, 10 in. wide,
and 11 in. with a plate 6 in. high by 6 in. wide behind it
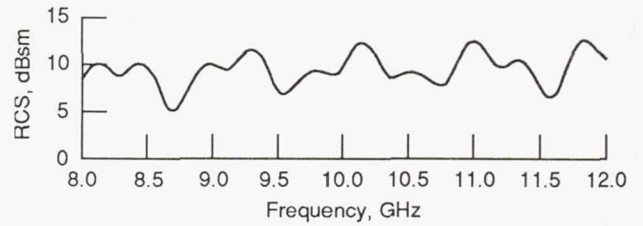at broadside incidence. The theoretical dielectric
constant is 1.093.

Figure 18.—Theoretical Radar Cross Section (RCS) of a
piece of shuttle tile material 5 3/16 in. thick, 10 in. wide,
and 11 in. with a plate 8 in. high by 8 in. wide behind it
at broadside incidence. The theoretical dielectric
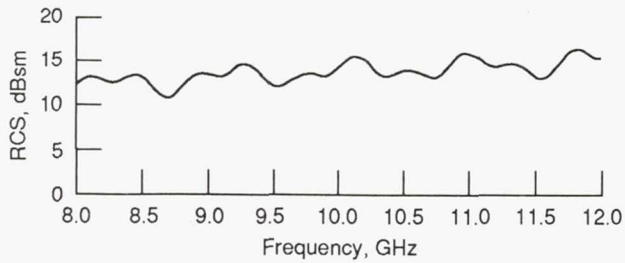constant is 1.093.

Figure 19.—Theoretical Radar Cross Section (RCS) of a
piece of shuttle tile material 5 3/16 in. thick, 10 in. wide,
and 11 in. with a plate 10 in. high by 10 in. wide behind
it at broadside incidence. The theoretical dielectric
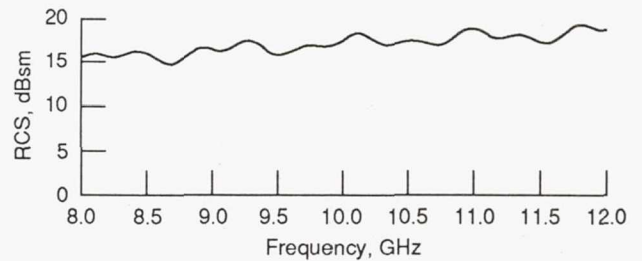constant is 1.093.

NASA
National Aeronautics and
Space Administration

Report Documentation Page

1. Report No. NASA CR-187140	2. Government Accession No.	3. Recipient's Catalog No.

4. Title and Subtitle	5. Report Date
Physical Optics for Oven-Plate Scattering Prediction	July 1991
	6. Performing Organization Code

7. Author(s)	8. Performing Organization Report No.
J. Baldauf, K. Lambert	None (E-6272)
	10. Work Unit No. 650-60-20

9. Performing Organization Name and Address	11. Contract or Grant No.
Analex Corporation 21775 Brookpark Road Brook Park, Ohio 44124	NAS3-25776
	13. Type of Report and Period Covered

12. Sponsoring Agency Name and Address	Contractor Report Final
National Aeronautics and Space Administration Lewis Research Center Cleveland, Ohio 44135-3191	14. Sponsoring Agency Code

15. Supplementary Notes

16. Abstract

This report describes an oven assembly design, which will be used to determine the effects of temperature on the electrical properties of materials which are used as coatings for metal plates. Experimentally, these plates will be heated to a very high temperature in the oven assembly, and measured using a microwave reflectance measurement system developed for the NASA Lewis Research Center, Near-Field Facility. One unknown in this measurement is the effect that the oven assembly will have on the reflectance properties of the plate. Since the oven will be much larger than the plate, the effect could potentially be significant as the size of the plate becomes smaller. Therefore, it is necessary to predict the effect of the oven on the measurement of the plate. This report will describe a method for predicting the oven effect, compare the theoretical oven effect to experimental results of the oven material, and describe the computer code which is used to predict the oven effect.

17. Key Words (Suggested by Author(s))	18. Distribution Statement
Physical optics Scattering prediction Scattering measurements	Unclassified - Unlimited Subject Category 33

19. Security Classif. (of the report)	20. Security Classif. (of this page)	21. No. of pages	22. Price*
Unclassified	Unclassified	14	A03

NASA FORM 1626 OCT 86   *For sale by the National Technical Information Service, Springfield, Virginia 22161

National Aeronautics and
Space Administration

Lewis Research Center
Cleveland, Ohio 44135

Official Business
Penalty for Private Use $300

FOURTH CLASS MAIL

ADDRESS CORRECTION REQUESTED

U.S.MAIL

NASA